available at www.sciencedirect.com

SCIENCE DIRECT®

journal homepage: www.elsevier.com/locate/biochempharm

Blockade of IGF-1 receptor tyrosine kinase has antineoplastic effects in hepatocellular carcinoma cells

Michael Höpfner [a], *Alexander Huether* [a], *Andreas P. Sutter* [a], *Viola Baradari* [a], *Detlef Schuppan* [b], *Hans Scherübl* [a,*]

[a] *Charité, Universitätsmedizin Berlin, Campus Benjamin Franklin, Medical Clinic I, Gastroenterology/Infectious Diseases/Rheumatology, 12200 Berlin, Germany*

[b] *Harvard Medical School, Beth Israel Deaconess Medical Center, Division of Gastroenterology and Hepatology, Boston, USA*

ARTICLE INFO

Article history:
Received 21 December 2005
Accepted 3 February 2006

Keywords:
IGF-1 receptor
Tyrosine kinase
Apoptosis
Cell cycle
EGFR
Cytostatics

Abbreviations:
TK, tyrosine kinase
MAPK, mitogen-activated protein kinase
PBS, phosphate-buffered NaCl solution
RT-PCR, reverse transcriptase-polymerase chain reaction
SDS, sodium dodecyl sulfate
PMSF, phenylmethylsulfonyl fluoride
ERK, extracellular signal-regulated kinase
BSA, bovine serum albumine
Tris, tris(hydroxymethyl)-aminomethane
MW, molecular weight

ABSTRACT

Hepatocellular carcinoma (HCC) is one of the most common cancer-related causes of death worldwide. Due to very poor 5-year-survival new therapeutic approaches are mandatory. Most HCCs express insulin-like growth factors and their receptors (IGF-R). As IGF-1R-mediated signaling promotes survival, oncogenic transformation and tumor growth and spread, it represents a potential target for innovative treatment strategies of HCC. Here we studied the antineoplastic effects of inhibiting IGF-1R signaling in HCC cells by the novel IGF-1R tyrosine kinase inhibitor NVP-AEW541.

Methods and results: NVP-AEW541 induced a time- and dose-dependent growth inhibition in the human hepatoblastoma and hepatocellular carcinoma cell lines SK-Hep-1, Hep-3B, Hep-G2 and Huh-7. Measurement of LDH-release showed that the antineoplastic effect of NVP-AEW541 was not due to cytotoxicity. Instead NVP-AEW541 induced apoptosis as evidenced by both caspase-3 and -8 activation as well as by apoptosis-specific morphological and mitochondrial changes. In addition, nuclear degradation was monitored by DNA-laddering. NVP-AEW541-treatment suppressed the expression of the antiapoptotic proteins Bcl-2 and survivin, while the expression of the proapoptotic protein BAX was stimulated in a dose-dependent manner. Moreover, NVP-AEW541 arrested the cell cycle at the G1/S checkpoint. When NVP-AEW541 was combined with cytotoxic chemotherapy or with a specific epidermal growth factor receptor antibody additive antiproliferative effects were observed.

Interpretation: Inhibition of IGF-1R tyrosine kinase (IGF-1R-TK) by NVP-AEW541 induces growth inhibition, apoptosis and cell cycle arrest in human HCC cell lines without accompanying cytotoxicity. Thus, IGF-1R-TK inhibition may be a promising novel treatment approach in HCC.

* *Corresponding author at*: Charité, Universitätsmedizin Berlin, Campus Benjamin Franklin, Medical Clinic I, Hindenburgdamm 30, 12200 Berlin, Germany. Tel.: +49 30 8445 3534; fax: +49 30 8445 4481.
E-mail address: hans.scherubl@charite.de (H. Scherübl).

0006-2952/$ – see front matter © 2006 Elsevier Inc. All rights reserved.
doi:10.1016/j.bcp.2006.02.006

HCC, hepatocelluar carcinoma
IGFR, insulin-like growth factor receptor
FADD, Fas associated death domain
Ψ, mitochondrial membrane potential
EGFR epidermal growth factor receptor
IGFBP, insulin-like growth factor binding protein
HEPES, *N*-(2-hydroxyethyl) piperazine-*N*′-(2-ethane-sulfonic acid)
DTT, dithiothreitol

1. Introduction

Hepatocellular carcinoma (HCC) is the one of the most common malignancies in the world with an estimated half a million deaths annually. The incidence of HCC is dramatically increasing in the USA, Europe and Asia, [1–4]. Curative ablation or resection of HCC, or liver transplantation can only be achieved in a minority of patients. Local tumor destruction, chemoembolisation and supportive therapy are the established treatment options in advanced HCC. However, overall survival is poor [5]. Therefore, innovative treatment approaches are urgently needed.

Recently, evidence has been accumulated that both insulin-like growth factors IGF-I and -II and their receptor tyrosine kinase, IGF-1R, are involved in the development and progression of cancer [6–8]. The human IGF-1R gene maps to chromosome 15q25-q26 and encodes a 1376 amino acid precursor that cleaves into a peptide-binding α-subunit and a β-subunit, which has intrinsic tyrosine kinase activity [9]. Interaction of IGF-I and -II with the IGF-1R plays a pivotal role in tumorigenesis, proliferation and spread of many cancers, by promoting cell cycle progression, preventing apoptosis, and by regulating and maintaining the tumorigenetic phenotype. Thus, not surprisingly, a wide variety of tumors including HCC show abnormal, or enhanced expression of IGFs and IGF-1R, which has been correlated with disease stage, reduced survival, development of metastases and tumor de-differentiation [10–12]. In addition to the increased expression of IGF-1R and IGFs a simultanous reduction of IGF binding protein expression (IGFBP) and enhanced proteolytic cleavage of IGFBP often occurs. Both mechanisms lead to an excessive increase in the amount of bioactive IGF [13,14], which further enhances the mito-oncogenic effects of IGFR-signaling in cancer cells. By contrast, the expression of IGF-1R is very low in normal hepatocytes whereas significant expression is achieved in Kupffer, endothelial and hepatic stellate cells. Thus, at least non-transformed hepatocytes are poorly responsive to IGFs [13].

Several approaches have demonstrated the therapeutic potential of interfering with IGF-1R mediated signaling in vitro and in vivo. These approaches included the use of IGF-1R blocking antibodies [15], IGF-1R antisense oligonucleotides [16] or IGF-1R siRNA [17]. Recently, potent and selective inhibitors of the IGF-1R tyrosine kinase (IGF-1R-TK) have been introduced as promising novel agents for cancer therapy. The orally available compound NVP-AEW541 is a low molecular weight inhibitor of IGF-1R-TK belonging to the pyrrolo[2,3-d]pyrimidine class. At the cellular level NVP-AEW541 was shown to be highly selective for IGF-1R-TK, as compared to both the closely related insulin receptor and other tyrosine or serine/threonine kinases. Antineoplastic properties of both NVP-AEW541 and of specific IGFR-antibodies have already been demonstrated in animal studies using a murine fibrosarcoma tumor model as well as in breast cancer and musculosceletal tumor cells in vitro [18,19].

In men, obesity and diabetes are clearly associated with an increased risk of hepatocellular cancer [4,20,21]. This effect seems to be due to alterations in the metabolism of endogenous hormones, including sex steroids, insulin and the IGF/IGFR system. Thus, a promising approach of innovative HCC treatment may be the blockade of the IGF/IGFR-signaling system, which is functionally expressed in HCC cells [13,22–24], and which has been shown to exert strong stimulatory effects on the growth of hepatoma cells [11]. The antineoplastic potency of IGFR-inhibition has already been demonstrated in several cancer models [25,26]. Importantly, IGFR-inhibition appears to be well-tolerated in prelimenary clinical studies [26]. However, IGFR-TK inhibition has not yet been evaluated for the treatment of HCC. Hence, in the present study we examined the antineoplastic potency of the selective IGF-1 tyrosine kinase inhibitor NVP-AEW541 in human hepatoblastoma and hepatocellular carcinoma cell lines. We provide evidence that NVP-AEW541 potently inhibits growth and induces both apoptosis and cell cycle arrest in human HCC cells.

2. Material and methods

2.1. Cell lines and drugs

The well differentiated wild-type p53 hepatoblastoma cell line Hep-G2 [27] and the highly differentiated, p53-mutated

human hepatocellular carcinoma cell line Huh-7 [28] were cultured in RPMI 1640 medium containing 10% fetal bovine serum and 100 U/ml penicillin and 100 mg/ml streptomycin. The human HCC cell lines Hep-3B (ATCC: #HB-8064) [29] and SK-Hep-1 [30] (ATCC: #HTB-52) were cultured in DMEM medium containing 10% fetal bovine serum, 100 U/ml penicillin, 100 mg/ml streptomycin and 2 mmol/l L-glutamine.

NVP-AEW541 was a kind gift from Novartis, Basel, Switzerland. Stock solutions were prepared in DMSO and stored at −20 °C and were diluted to the final concentration in fresh media before each experiment. The monoclonal EGFR-antibody Ab-3103 was purchased from Abcam (Cambridge, UK). In all experiments, the final DMSO concentration was <0.5%.

To evaluate the effects of NVP-AEW541, cells were incubated with either control medium or medium containing rising concentrations of NVP-AEW541. Media were changed every second day to ensure constant drug concentrations in the incubation medium.

2.2. RT-PCR

Total RNA was extracted from cultured cell lines with RNAClean following the recommendation of the manufacturer (Hybaid, London, UK). To eliminate any possible contamination with genomic DNA, RNAs were treated with 1 U DNAse per μg RNA for 15 min at room temperature and were then reverse transcribed into cDNA using oligo-dT-primers and the SuperScript Preamplification-Kit following the manufacturers' instructions (Gibco). PCR reactions were carried out in a total volume of 50 μl containing 400 nM of each primer, 200 μM of each dNTP (Pharmacia, Uppsala, Sweden), 50 mM KCl, 1.5 mM $MgCl_2$, 10 mM Tris and 1 U Taq-Polymerase (Pharmacia). PCR was performed in a Peltier thermocycler (PTC-200, MJ Research, Watertown, MA) with established primers and conditions [31].

2.3. Measurement of growth inhibition

Cell number was evaluated by crystal violet staining, as described [32]. Cells cultured in 96-well plates were fixed with 1% glutaraldehyde and stained with 0.1% crystal violet. The unbound dye was removed by washing with water. Bound crystal violet was solubilized with 0.2% Triton-X-100. Light extinction which increases linearly with the cell number was analyzed at 570 nm using an ELISA-Reader.

2.4. Functional detection of apoptosis

Changes in mitochondrial membrane potential ($\Delta\Psi_M$) and mitochondrial volume were assessed as described [33]. Cells were stained using the fluorogenic lipophilic cation 5,5′,6,6′-tetrachloro-1,1′,3,3′-tetraethyl-benzimidazolylcarbocyanine iodide (JC-1, 1 μg/ml, Molecular Probes, Eugene, OR) for 15 min at 37 °C in the dark, prior to analysis by flow cytometry. JC-1 is capable of selectively entering the mitochondria, where it changes its color from green to orange as the membrane potential increases due to apoptotic events. This property is due to the reversible formation of JC-1 aggregates upon membrane polarization that causes shifts in emitted light from 530 nm (emission of JC-1 monomeric form) to 590 nm (emission of J-aggregates) when excited at 490 nm.

Preparation of cell lysates and determination of caspase activity was performed as described previously [34]. The activity of caspases was calculated from the cleavage of fluorogenic substrates (caspase-3: DEVD-AMC; caspase-8: Z-IETD-AFC, Calbiochem-Novabiochem, Bad Soden, Germany). To monitor caspase-3-independent caspase-8 activation, the specific caspase-3 inhibitor 5-[(S)-(−)-2-(methoxymethyl)pyrrolidino]-sulfonylisatin (Calbiochem) was used in a subset of experiments [35]. Cell lysates were incubated with caspase substrate solution (20 μg/ml of either caspase-3 or -8 substrate, HEPES 20 mM, glycerol 10%, DTT 2 mM, pH 7.5) for 1 h at 37 °C, and the substrate cleavage was measured fluorometrically with a VersaFluor fluorometer from Biorad, Munich, Germany.

DNA fragmentation was determined by using a DNA laddering kit (Roche) according to the manufacturers' instructions. After cell lyses samples were poured into centrifugation tubes containing glass fibre fleece which binds the apoptotic DNA in the presence of guanidine hydrochloride. After centrifugation and additional washing steps, apoptotic DNA was eluted and collected by centrifugation. Purified DNA (2 μg/sample) was mixed with gel loading buffer and analyzed on an agarose gel.

2.5. Determination of cell viability and apoptosis-specific cellular morphology

Cell viability was measured with a cell viability/cytotoxicity assay kit (LIVE/DEAD assay) from Molecular Probes (Leiden, The Netherlands) as described elsewhere in detail [36]. After 24 h of incubation with NVP-AEW541 (0–10 μM) in the presence or absence of caspase-3 inhibitor (0.5 μg/ml), cells were incubated with 160 nM calcein-AM and 2 μM EthD-1 (1 h; 37 °C) and examined by fluorescence microscopy. Live cells were identified by the presence of ubiquitous intracellular esterase activity leading to the conversion of non-fluorescent cell-permeable calcein-AM to the green-fluorescent polyanionic dye calcein (ex/em ~495/~510 nm), which is well retained within live cells. Dead cells were determined by EthD-1 (ex/em ~495/~635 nm), which becomes red-fluorescent upon binding to nucleic acids of cells with dameged membranes. Quantification of live and dead cells in each sample was done by calculating the average value of at least four arbitrarily chosen image areas of a respective coverslip.

2.6. Determination of cytotoxicity

Five thousand cells/well were seeded into 96-well microtiter plates and incubated with NVP-AEW541. Release of cytotoxicity indicating lactate dehydrogenase (LDH) was measured after 6 and 24 h of incubation by using a colorimetric kit from Roche as described elsewhere [37]. Maximum release of LDH was obtained by adding 100 μl of 2% Triton X-100 to untreated cells. One-hundred microlitres of each sample were incubated with 100 μl of LDH assay reagent for

10 min. Thereafter the absorbance of samples was measured at 490 nm. Percentage of LDH release was determined by dividing released LDH of the cells by maximum LDH release multiplied by 100. No significant amount of LDH was detected in the tissue culture medium alone nor in NVP-AEW541-containing incubation medium.

2.7. Cell cycle analysis

Cell cycle analysis was performed by the method of Vindelov and Christensen, as described previously [38,39]. Cells were trypsinized, washed, and the nuclei were isolated using CycleTest PLUS DNA Reagent Kit (Becton Dickinson, Heidelberg, Germany). DNA was stained with propidium iodide according to the manufacturers' instructions. The DNA content of the nuclei was detected by flow cytometry and analyzed using CellFit software (Becton Dickinson, Heidelberg, Germany).

2.8. Western blotting

Western blotting was performed as described [40,41]. Whole-cell extracts were prepared by lysing cells. Lysates containing 30 μg protein were subjected to gel electrophoresis. Proteins were then transferred to PVDF membranes by electroblotting for 2 h. Blots were blocked in 1% non-fat dry milk for 30 min, and then incubated at 4 °C overnight with anti-human Bcl-2 or BAX (1:200 or 1:1000, Novo Castra Laboratories, Newcastle, UK) or survivin (1:300, Santa Cruz Biotechnology, CA, USA) antibodies, respectively. For detection of IGF-1R protein expression a polyclonal antibody (1:1000, Santa Cruz Biotechnology, CA, USA), recognizing the β-chain of IGF-1R was used [31]. COX-2 expression was investigated by using a monoclonal COX-2 antibody (1:400, Santa Cruz Biotechnology, CA, USA).

After incubation with horseradish peroxidase-coupled anti-IgG antibody (1:10,000, Amersham, Uppsala, Sweden) at room temperature for 1 h, the blot was developed using enhanced chemiluminescent detection reagent (Amersham) and subsequently exposed to Hyperfilm ECL film (Amersham) for 0.5–5 min. Experiments were performed three times, and respresentative experiments are shown.

2.9. Statistical analysis

If not stated otherwise, means of four independent experiments ± S.E.M. are shown. Individual drug treatment was compared by the unpaired, two-tailed Mann–Whitney *U*-test. *P* values were considered to be significant at <0.05.

3. Results

3.1. Expression of IGF-1R in hepatocellular carcinoma

mRNA expression of the insulin-like growth factor receptor 1 (IGF-1R) was investigated in the human hepatoblastoma and hepatocelluar carcinoma cell lines Huh-7, Hep-G2, Hep-3B and SK-Hep-1. Robust expression of mRNAs specific for IGF-1R was detected in all cell lines (Fig. 1A). To evaluate the protein expression of IGF-1R, Western blot analysis was performed. Both the IGF-1R precursor that cleaves into α- and

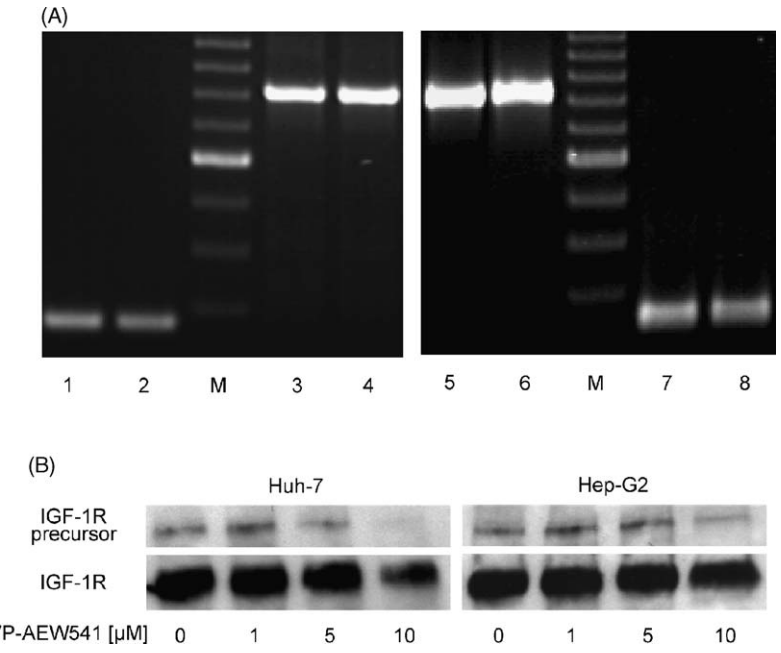

Fig. 1 – Expression of IGF-1R in hepatocellular carcinoma. (A) mRNA expression of IGF-1R (amplicon size: 241 bp) in Hep-3B (lane 1), SK-Hep-1 (lane 2), Hep-G2 (lane 7) and Huh-7 (lane 8) cells. The expression of the housekeeping gene β-actin (amplicon size: 822 bp) in Hep-3B (lane 3), SK-Hep-1 (lane 4), Hep-G2 (lane 4) and Huh-7 (lane 5) cells was analyzed for standardization. M: 100 bp DNA ladder. (B) Expression of IGF-1R and IGF-1R-precursor protein was evaluated in NVP-AEW541-treated (0–10 μM for 24 h) Huh-7 (left side) and Hep-G2 (right side) cells by Western Blot. Both cell lines showed a robust expression of IGF-1R protein.

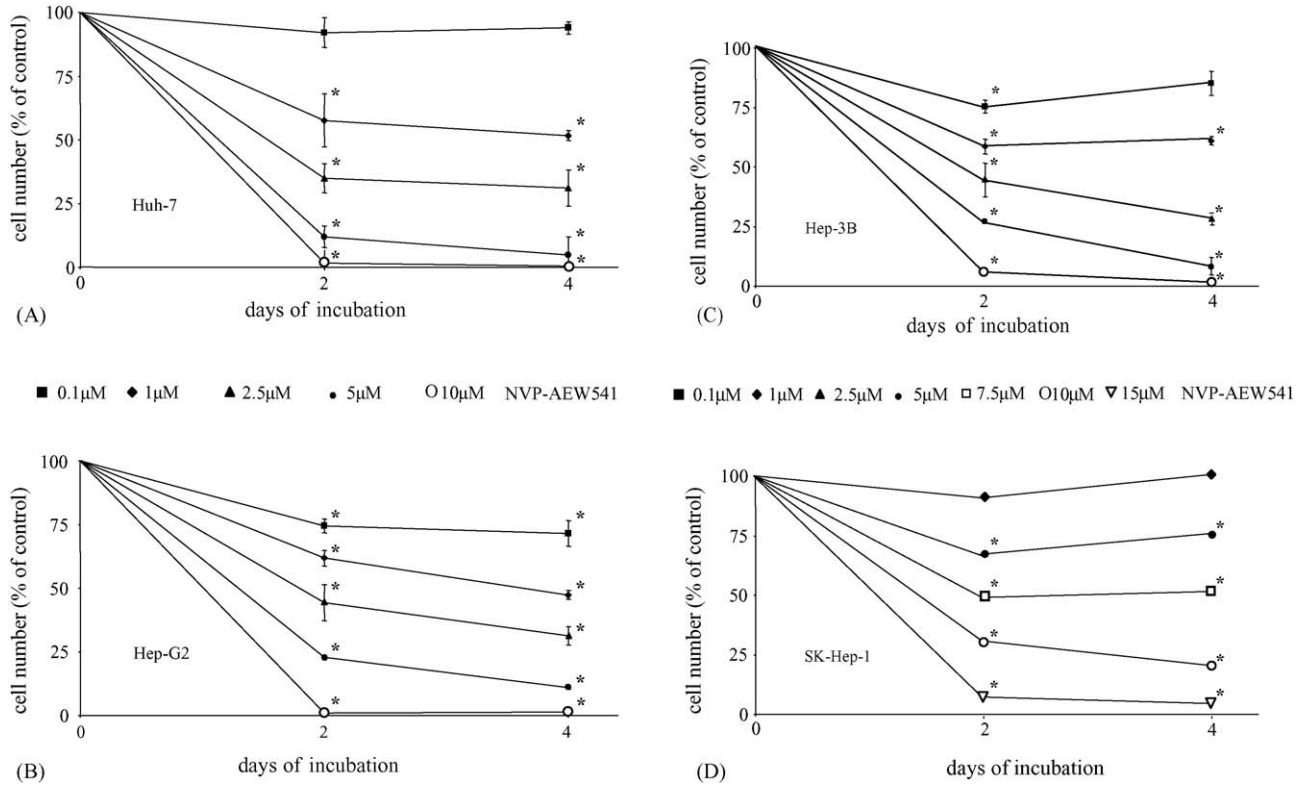

Fig. 2 – NVP-AEW541-induced growth inhibition. NVP-AEW541 caused a time- and dose-dependent growth inhibition of HCC cells, as measured by crystal violet staining. The IC_{50} value amounted to 1.8 ± 0.3 μM (Hep-G2, 2a), 1.4 ± 0.2 μM (Huh-7, 2a), 1.9 ± 0.3 μM (Hep-3B, 2c) and 6.9 ± 0.5 μM (SK-Hep-1, 2d) cells. Data are given as percentage of untreated controls (means ± S.E.M. of four independent experiments). *, Statistical significance ($p < 0.05$), compared to untreated controls.

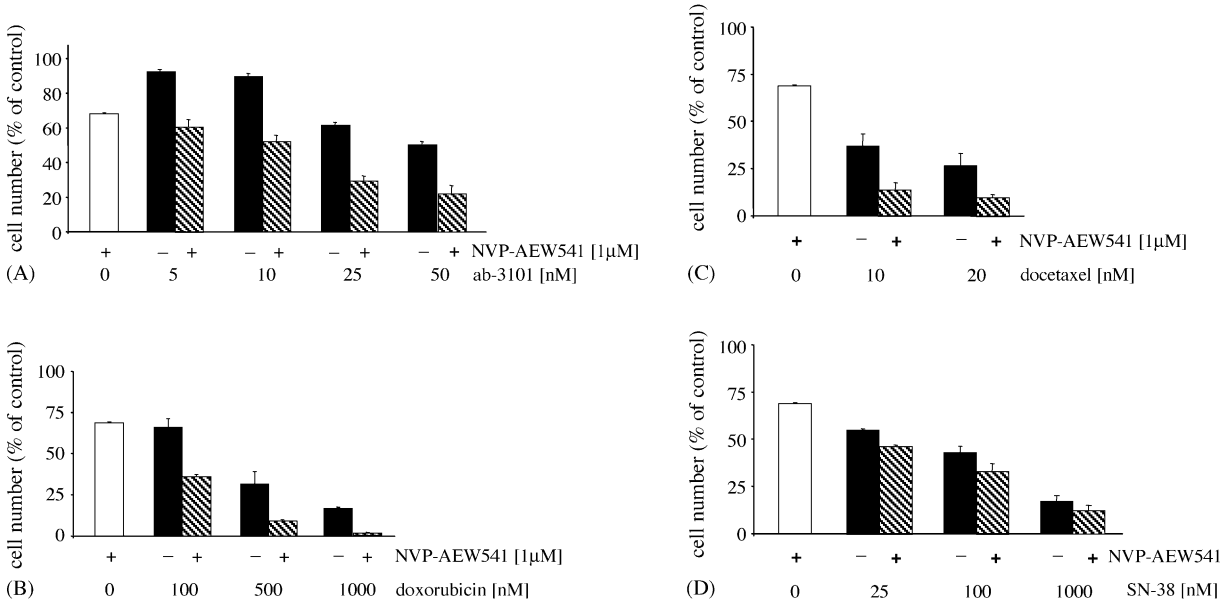

Fig. 3 – Antiproliferative effects of NVP-AEW541-based combination treatments. Hepatocelluar carcinoma Huh-7 cells were treated for 72 h with rising concentrations of the EGFR-antibody, Ab-3101 (A), doxorubicin (B), docetaxel (C), or SN-38 (D) alone (black bars) or in combination with with 1 μM NVP-AEW541 (hatched bars). White bars show the effects of 1 μM NVP-AEW541 alone. Data are given as percentage of untreated controls, which were set at 100%. Means ± S.E.M. of three to five independent experiments.

β-subunits as well as the β-chain of the mature form of IGF-1R were evaluated in Huh-7 and Hep-G2 cells (Fig. 1B). Incubation with rising concentrations of NVP-AEW541 (0–10 μM) for 24 h did not abolish the marked expression IGF-1R protein.

3.2. Growth inhibitory effects of NVP-AEW541

IGF-1R-TK inhibition with NVP-AEW541 time- and dose-dependently inhibited the growth of all four HCC cell lines (Fig. 2A–D). After 96 h of incubation with rising concentrations of NVP-AEW541 a decrease in cell number by almost 100% was observed. The IC_{50} values of NVP-AEW541 determined after 48 h were 1.4 ± 0.2 μM (Huh-7), 1.8 ± 0.3 μM (Hep-G2) 1.9 ± 0.3 μM (Hep-3B) and 6.9 ± 0.5 μM in SK-Hep-1 cells.

Recently, we and others showed that a coexpression of IGF-1R together with the epidermal growth factor receptor (EGFR) might be critical for EGFR-dependent mitogenic effects [31], since IGF-1R is capable of transactivating EGFR-TK activity [42]. We demonstrated previously that HCC cells express EGFR [41,43]. Therefore we investigated the effects of a combined treatment of HCC cells with NVP-AEW541 *plus* the monoclonal EGFR-blocking antibody ab-3101. Applying ab-3101 (1–50 nM) alone for 3 days decreased the growth of Huh-7 cells by up to 52 ± 1.8%. Combinations of ab-3101 and 1 μM NVP-AEW541 resulted in additive growth inhibitory effects of up to 80%, as compared to untreated controls (Fig. 3A). Additive antiproliferative effects were also observed when NVP-AEW541 was combined with the two clinically relevant chemotherapeutic agents doxorubicin or docetaxel (Fig. 3B and C). By contrast, the antiproliferative effect of SN-38 was not markedly enhanced by co-treatment with NVP-AEW541 (Fig. 3D).

3.3. NVP-AEW541 and cell cycle regulation

To test whether induction of cell cycle arrest contributed to the antiproliferative potency of NVP-AEW541 in hepatocellular cancer cells, we performed flow cytometric cell cycle analysis. Twenty four hours of incubation with rising concentrations of NVP-AEW541 dose-dependently arrested HCC cells in the G1/G0 phase of the cell cycle, thereby decreasing the proportion of cells in the S-phase. Moreover, especially in Huh-7 cells an apoptosis-specific increase of the sub-G1-peak was observed at higher concentrations (Fig. 4).

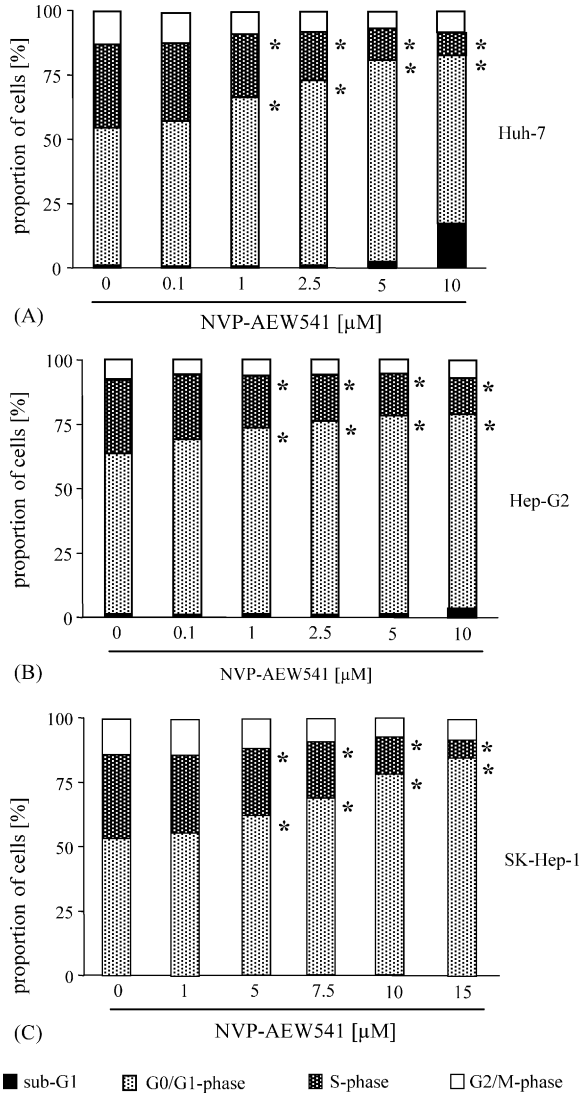

Fig. 4 – Induction of cell cycle arrest by NVP-AEW541. After 24 h of incubation with NVP-AEW541 Huh-7 (A), Hep-G2 (B), and SK-Hep-1 (C) cells dose-dependently accumulated in the G0/G1-phase of the cell cycle. Accordingly, the proportion of cells in the S- and G2/M-phase decreased. At high concentrations NVP-AEW541 additionally induced an apoptosis-specific increase in the proportion of sub-G1 cells of Huh-7 and Hep-G2 cells (SK-Hep-1: not determined). Means of four independent experiments are shown. The difference of the proportion of cells in a particular phase of the cell cycle versus control was significant for 1–10 μM of NVP-AEW541 in Huh-7 and Hep-G2 cells, and 5–15 μM in SK-Hep-1 cells. *, Statistical significance ($p < 0.05$).

3.4. Proapoptotic effects of NVP-AEW541

To further investigate NVP-AEW541-induced apoptosis in HCC cells, changes in mitochondrial membrane potential (Ψ_M) and mitochondrial volume by NVP-AEW541 were determined. Incubation with rising concentrations of NVP-AEW541 for 3, 6, 12 and 24 h led to a time- and dose-dependent drop in Ψ_M, suggesting the mitochondrium to be involved in NVP-AEW541-induced apoptosis of hepatocellular carcinoma cells (Fig. 5). Interestingly, neither in Huh-7 nor Hep-G2 cells was a marked increase in mitochondrial volume detected. Even at the highest concentration of 10 μM NVP-AEW541 only a small increase of less than 20% was observed.

Next, we evaluated the activation of caspase-3, a key enzyme in the apoptotic signaling cascade. In Huh-7 cells NVP-AEW541 (0–10 μM) induced a dramatic 27-fold increase in caspase-3 activity after 24 h of incubation.

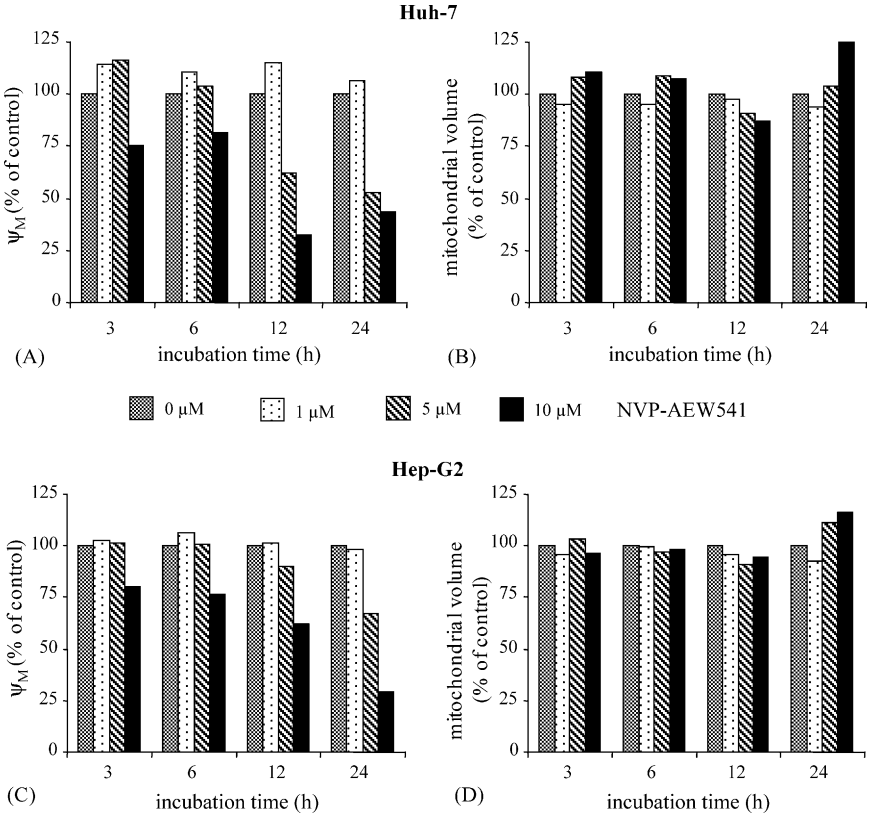

Fig. 5 – NVP-AEW541-induced mitochondrial changes. To monitor changes in the mitochondrial membrane potential ($\Delta\Psi_M$) the mitochondria of Huh-7 and Hep-G2 cells were stained with JC-1 and analyzed by flow cytometry. After 3–24 h of incubation with NVP-AEW541 (0–10 μM) Huh-7 (A) cells and Hep-G2 (C) cells showed a time- and dose-dependent depolarization of $\Delta\Psi_M$. By contrast, neither Huh-7 cells (B) nor Hep-G2 cells (D) displayed a marked increase in mitochondrial volume after incubation with NVP-AEW541. Data are given as percentage of untreated control (means ± S.E.M. of three independent experiments for each cell line).

Dose-dependent increases in caspase-3 activity were also observed in Hep-G2, Hep-3B and SK-Hep-1 cells (Fig. 6A–D).

Caspase-3 can be activated by either mitochondrial-dependent or -independent signaling events. Therefore, we additionally checked for the activation of caspase-8 being implicated in mitochondria-independent caspase-3 activation. Challenging HCC cells with 0–10 μM NVP-AEW541 for 24 h led to a dose-dependent increase in caspase-8 in HCC cell lines (Fig. 6E and F). To evaluate, whether the observed activation of caspase-8 was induced by caspase-3, which has recently been described as a reinforcing feedback mechanism of mitochondria-dependent caspase-3 activation [44], we performed additional experiments with a specific caspase-3 inhibitor. The experiments clearly demonstrated that no mitochondria-independent induction of apoptosis by caspase-8-dependent signaling occurred, as caspase-3 inhibition almost completely abolished caspase-8 activation. To further substantiate NVP-AEW541-induced apoptosis cells we also determined the fragmentation of the DNA in hepatocellular Huh-7 carcinoma cells after 24 h incubation with 10 μM NVP-AEW541 (Fig. 6G).

3.5. *Cytoxicity of NVP-AEW541*

Cytotoxicity was determined by measuring LDH release. Incubating Hep-G2, Huh-7 and SK-Hep-1 cells with NVP-AEW541 for 6 h did not result in any measureable increase of LDH release (Fig. 7), indicating that NVP-AEW541 does not directly affect cell membrane integrity and does not have immediate cytotoxic effects even at high concentrations. However, after 24 h an increase in LDH release of up to 30% above control levels was observed in Huh-7 cells treated with 10 μM NVP-AEW541. To further evaluate whether this increased LDH release actually reflected cytotoxicity of NVP-AEW541, we additionally performed LIVE/DEAD-fluorescence microscopy. The experiments revealed that NVP-AEW541-treated cells underwent dramatic morphological changes, which included the formation of apoptotic bodies and the fragmentation of nuclei. Cells appeared unstructured, shrunken and flat and displayed morphological signs of apoptosis (Fig. 8). Co-incubation of NVP-AEW541 together with a caspase-3 inhibitor (0.5 μg/ml) almost completely abolished these morphological changes and no NVP-AEW541-induced increase in cell death was still observed. This finding was confirmed by additional LDH release measurements.

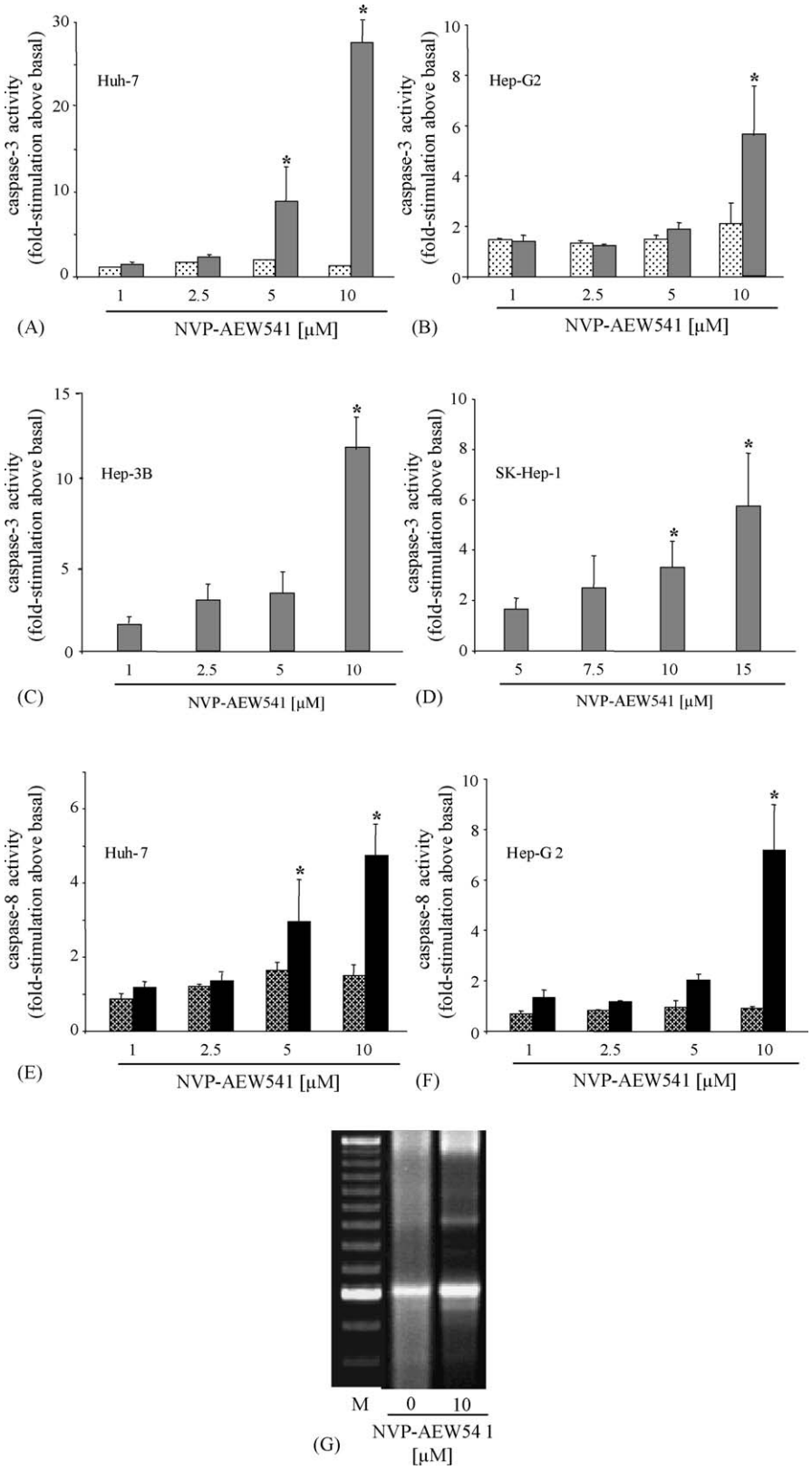

Fig. 6 – NVP-AEW541-induced activation of caspases and DNA fragmentation. NVP-AEW541-induced activation of caspases-3 and -8 was evaluated in HCC cells. (A–D) Upon NVP-AEW541-treatment caspase-3 was dose-dependently activated in Huh-7 (A), Hep-G2 (B), Hep-3B (C) and SK-Hep-1 (D) cells. As shown for Huh-7 (A) and Hep-G2 cells (B) the effect was completely abolished, when the cells were co-treated with a caspase-3 inhibitor (dotted bars). (E, F) Dose-dependent caspase-8 activation by NVP-AEW541 in Huh-7 (E) and Hep-G2 (F) cells was completely abolished, when the cells were co-treated with a caspase-3 inhibitor (hatched bars), indicating caspase-3-dependent caspase-8 activation. Data are given as

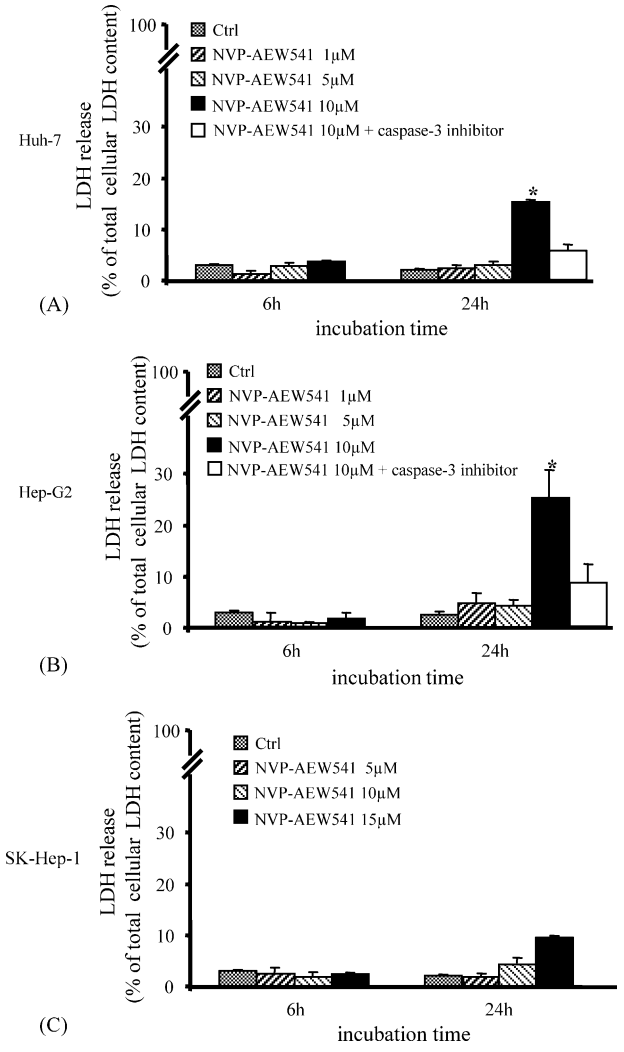

Fig. 7 – NVP-AEW541 induced cytotoxicity. LDH release into the supernatant of Huh-7 (A), Hep-G2 (B) and SK-Hep-1 (C) cells was determined after incubation with rising concentrations of NVP-AEW541. No significant LDH release was observed during the first hours of incubation. After 24 h only 10 μM NVP-AEW541 led to an increase in LDH release. Co-incubation with a caspase-3 inhibitor almost completely abolished the NVP-AEW541-induced LDH release, as determined for Huh-7 (A) and HEP-G2 (B) cells. Data of 4 independent experiments ± S.E.M. are shown. *, Statistical significance ($p < 0.05$) compared to untreated controls.

Co-administration of the caspase-3 inhibitor (0.5 μg/ml) together with NVP-AEW541 (10 μM) abrogated NVP-AEW541-induced LDH release after 24 h of incubation (Fig. 7A and B). Hence, NVP-AEW541 induced LDH release was likely to occur due to secondary necrosis following the pronounced induction of apoptosis by NVP-AEW541.

3.6. NVP-AEW541 regulates the expression of BAX, Bcl-2, survivin and COX-2

To elucidate the signaling pathways modulated by IGF-1R-TK inhibition in HCC cells, we investigated changes in the expression of apoptosis-specific proteins. Incubating HCC cells for 24 h with rising concentrations of NVP-AEW541 revealed a time- and dose-dependent increase in the expression of the proapoptotic BAX protein, while the expression of the antiapoptotic proteins Bcl-2 and survivin decreased (Fig. 9). Moreover, 72 h incubation of HCC cells with NVP-AEW541 (1.5 and 3 μM) led to a dose-dependent decrease in COX-2 expression (data not shown).

4. Discussion

In the present study we provide evidence that the highly specific IGF-1R tyrosine kinase inhibitor NVP-AEW541 potently inhibits the growth of hepatocellular carcinoma cells. The antineoplastic actions of NVP-AEW541 comprised both cell cycle arrest and induction of apoptosis. No appreciable induction of cytotoxicity was observed, indicating that NVP-AEW541 does not act in an ''unspecific'' cytotoxic way.

It has been pointed out that the antiapoptotic potency of IGF/IGFR-signaling might interfere with strategies that target other tyrosine kinases such as the epidermal growth factor receptor (EGFR)-tyrosine kinase (EGFR-TK). EGFR-TK inhibition has already been reported to potently inhibit the proliferation of hepatocellular cancer cells in vitro and in vivo [41,43,45,46]. However, the antineoplastic potency of EGFR blockade may well be underestimated when examined under conditions where IGF-1R is fully functional, since IGF-1R is capable of transactivating EGFR-TK [42,47]. Transactivation of EGFR-TK by IGFR has already been demonstrated to decrease the antiproliferative effects of EGFR-antibody treatment [48].

Here we studied the effects of combination treatments with the EGFR-antibody ab-3101 and NVP-AEW541. Treating HCC cells with sub-IC_{50} concentrations of NVP-AEW541 and ab-3101 additively enhanced the antiproliferative effect of either agent alone. Hence, dual-targeting of both IGF-1R and EGFR may be a promising approach for enhanced treatment efficacy as it overcomes compensatory effects of mitogenic crosstalks between IGF-1R and EGFR. In this respect Lu and co-workers recently reported on a sucessful dual-targeting of IGF-1R and EGFR by use of a bispecific antibody, which markedly exceeded the antineoplastic potency of the blockade of either EGFR or IGFR alone [49].

Chemotherapeutic agents with different modes of action were also evaluated for combination treatment with NVP-AEW541. Combinations of NVP-AEW541 plus the topoisomerase II inhibitor, doxorubicin, or plus the antimicrotubule agent docetaxel resulted in a doubling of the growth inhibitory effects that were achieved in monotherapeutic approaches with either chemotherapeutic agent.

percentage of untreated control (means ± S.E.M. of four independent experiments for each cell line). (G) After 24 h of incubation NVP-AEW541 (10 μM) caused apoptosis-specific fragmentation of cellular DNA of Huh-7 cells. M = 100 bp marker. Representative tracing out of three independent experiments. *, Statistical significance ($p < 0.05$), compared to untreated controls.

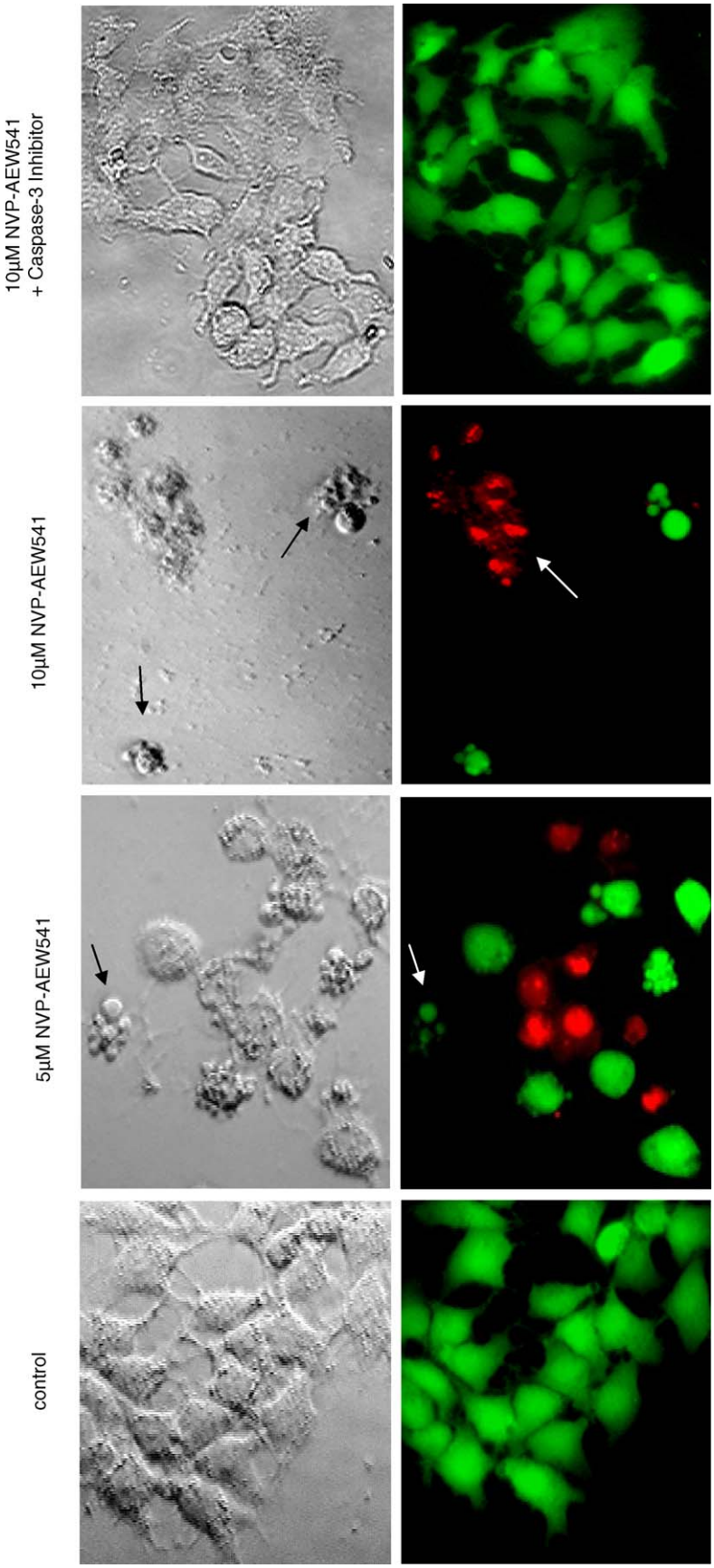

Fig. 8 – NVP-AEW541-induced cell death of hepatocellular carcinoma cells. NVP-AEW541-mediated induction of cell death and apoptosis-specific morphological changes of Huh-7 cells were determined by LIVE/DEAD-fluorescence microscopy.

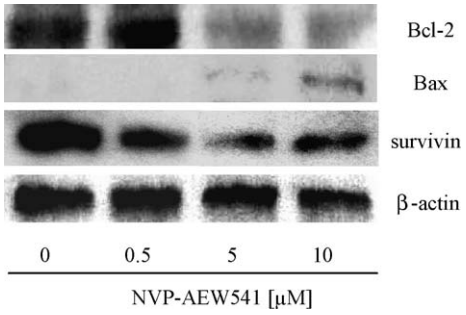

Fig. 9 – Effects of NVP-AEW541 on the expression of the apoptosis-relevant proteins BAX, Bcl-2 and survivin. Huh-7 cells were treated with rising concentrations of NVP-AEW541 (0–10 μM) for 24 h. Changes in the expression of Bcl-2, BAX and survivin were analyzed by Western blotting. NVP-AEW541 induced a dose-dependent decrease of the antiapoptotic proteins Bcl-2 and survivin, while the expression of the proapoptotic BAX protein increased. Representative results out of three independent experiments are shown.

To characterize the underlying mechanisms of NVP-AEW541's antineoplastic action, we performed cell cycle analysis. Upon NVP-AEW541-treatment the proportion of cells in the G1/G0-phase significantly increased in the investigated cell lines, suggesting that NVP-AEW541 acts at the G1/S checkpoint. A G1/S cell cycle arrest induced by inhibition of IGFR-signaling has been described for other fast growing cancers [6,50]. Cell cycle analysis of HCC cells also revealed a first hint for the induction of apoptosis by NVP-AEW541. Especially at high NVP-AEW541 concentrations a marked increase in the apoptosis-indicating sub-G1-peak became apparent. Induction of apoptosis by inhibition of IGFR-signaling has been reported previously [24,51–53]. However, the underlying mechanisms have not been elucidated in detail yet. By determining morphological and functional changes, caspase-3 and -8 activation as well as the fragmentation of nuclear DNA we demonstrated the ability of NVP-AEW541 to potently induce apoptosis in HCC cells. The observed sequence of events suggests that NVP-AEW541-mediated apoptosis of HCC cells is caspase-3-dependent, because on the one hand caspase-3 activation preceeded fragmentation of cellular DNA and on the other hand the apoptotic effects of NVP-AEW541 were completely abolished by caspase-3 inhibition.

Since the activation of this executioner caspase can be induced by mitochondria-dependent and/or -independent pathways, we investigated the underlying signaling events. Previous studies indicated that a decrease of the inner transmembrane potential with a concomitant increase of the permeability of the outer mitochondrial membrane by opening the permeability transition pore constituted the initial step of mitochondria-mediated apoptosis [40,54,55]. Indeed, upon NVP-AEW541-treatment we observed a time- and dose-dependent decrease of the mitochondrial membrane potential ($\Delta\Psi_M$) but we could not detect a pronounced mitochondrial swelling. Interestingly, Gogvadze and co-workers recently reported that BAX-driven apoptosis might occur without changes in mitochondrial volume [56]. Investigating NVP-AEW541-induced BAX expression by Western blotting, we found a dose-dependent upregulation of BAX by NVP-AEW541, arguing for the involvement of BAX in NVP-AEW541-induced apoptosis. Moreover, we observed a downregulation of Bcl-2 by NVP-AEW541 which further supports the notion that the mitochondria are involved in the activation of caspase-3.

Recently, we and others demonstrated that inhibition of growth factor receptor signaling resulted in death receptor- and mitochondria-independent apoptosis, still involving the activation of the initiator caspase-8 [41,57]. In the present study we also observed an activation of caspase-8 by NVP-AEW treatment. Caspase-8 activation may occur independently of Fas or other TNF family death receptors [58–64], but may also depend on caspase-3 activation, which has been described as a feedback mechanism for the reinforcement of mitochondria-dependent apoptosis [44]. Our findings on NVP-AEW541-induced apoptosis of HCC cells suggest that the latter case applies for the observed caspase-8 activation by NVP-AEW541, as it was almost completely abolished in the presence of a caspase-3 inhibitor.

Finally, we observed a downregulation of the antiapoptotic protein survivin upon NVP-AEW541-treatment. This effect is of particular interest, since Morinaga and co-workers recently showed that mRNA expression of survivin was significantly related to the histologic grade and pathological tumor stage of clinical HCC, indicating that survivin was associated with reduced tumor cell apoptosis, increased tumor cell proliferation, and aggressive tumor features [65]. In this line, survivin expression is known to correlate with aggressive tumor biology in various gastrointestinal cancers [66]. In addition, NVP-AEW541 downregulated the expression of cyclooxygenase-2 (COX-2) in HCC cells. COX-2 is known to be upregulated during hepatocarcinogenesis and plays an important role in HCC growth. Thus, the effects of NVP-AEW541 on survivin and COX-2 expression may well contribute to its antineoplastic potency in HCC disease.

Our study provides first evidence that the IGFR-TK inhibitor NVP-AEW541 potently inhibits the growth of human hepatoblastoma and hepatocellular cancer cells by inducing both cell cycle arrest and apoptosis without accompanying cytotoxicity. Our promising in vitro-data merit in vivo-verification to check-out the clinical suitability of NVP-AEW541 for HCC treatment. Moreover, future investigations should be pursued

Viable cells are stained green, while cells with impaired cell membrane appeared. Phase-contrast images are shown in the upper panel, the corresponding fluorescence micrographs in the lower panel. NVP-AEW541 dose-dependently induced an increase in cell death and apoptosis-specific formation of apoptotic bodies (black arrows) as well as DNA-fragmentation (white arrow). In the presence of a caspase-3-inhibitor the effects of NVP-AEW541 were completely abolished. Representative findings of $n = 4$ independent experiments. $*$, Statistical significance ($p < 0.05$), compared to untreated controls.

to modulate the IGF/IGFR-system as a possible means of HCC prevention in patients at risk.

Acknowledgements

We are indebted to Anje Krahn for expert technical assistance. We thank Novartis Pharma for providing us with NVP-AEW541. A. Huether and Viola Baradari were supported by scholarships from the Sonnenfeld-Stiftung, Berlin and the Deutsche Forschungsgemeinschaft, respectively. We thank the Institute of Physiology, Charité, Universitätsmedizin Berlin, Campus Benjamin Franklin, for lab facilities.

REFERENCES

[1] El Serag HB, Davila JA, Petersen NJ, McGlynn KA. The continuing increase in the incidence of hepatocellular carcinoma in the United States: an update. Ann Intern Med 2003;139:817–23.
[2] McGlynn KA, Tsao L, Hsing AW, Devesa SS, Fraumeni Jr JF. International trends and patterns of primary liver cancer. Int J Cancer 2001;94:290–6.
[3] Yu MC, Yuan JM. Environmental factors and risk for hepatocellular carcinoma. Gastroenterology 2004;127:72–8.
[4] Caldwell SH, Crespo DM, Kang HS, Al-Osaimi AM. Obesity and hepatocellular carcinoma. Gastroenterology 2004;127:97–103.
[5] El Serag HB, Mason AC, Key C. Trends in survival of patients with hepatocellular carcinoma between 1977 and 1996 in the United States. Hepatology 2001;33:62–5.
[6] Baserga R. Oncogenes and the strategy of growth factors. Cell 1994;79:927–30.
[7] Wang Y, Sun Y. Insulin-like growth factor receptor-1 as an anticancer target: blocking transformation and inducing apoptosis. Curr Cancer Drug Targets 2002;2:191–207.
[8] Wang Z, Ruan YB, Guan Y, Liu SH. Expression of IGF-II in early experimental hepatocellular carcinomas and its significance in early diagnosis. World J Gastroenterol 2003;9:267–70.
[9] Ulrich A, Gray A, Tam AW, Yang-Feng T, Tsubokawa M, Collins C, et al. Insulin-like growth factor I receptor primary structure: comparison with insulin receptor suggests structural determinants that define functional specificity. EMBO J 1986;5:2503–12.
[10] Sedlaczek N, Hasilik A, Neuhaus P, Schuppan D, Herbst H. Focal overexpression of insulin-like growth factor 2 by hepatocytes and cholangiocytes in viral liver cirrhosis. Br J Cancer 2003;88:733–9.
[11] Scharf JG, Braulke T. The role of the IGF axis in hepatocarcinogenesis. Horm Metab Res 2003;35:685–93.
[12] Yao X, Hu JF, Daniels M, Yien H, Lu H, Sharan H, et al. A novel orthotopic tumor model to study growth factors and oncogenes in hepatocarcinogenesis. Clin Cancer Res 2003;9:2719–26.
[13] Alexia C, Fallot G, Lasfer M, Schweizer-Groyer G, Groyer A. An evaluation of the role of insulin-like growth factors (IGF) and of type-I IGF receptor signaling in hepatocarcinogenesis and in the resistance of hepatocarcinoma cells against drug-induced apoptosis. Biochem Pharmacol 2004;68:1003–15.
[14] Yu H, Rohan T. Role of the insulin-like growth factor family in cancer development and progression. J Natl Cancer Inst 2000;92:1472–89.
[15] Scotlandi K, Benini S, Nanni P, Lollini PL, Nicoletti G, Landuzzi L, et al. Blockage of insulin-like growth factor I receptor inhibits the growth of Ewing's sarcoma in athymic mice. Cancer Res 1998;58:4127–31.
[16] Shapiro DN, Jones BG, Shapiro LH, Dias P, Houghton PJ. Antisense-mediated reduction in insulin-like growth factor-I receptor expression suppresses the malignant phenotype of a human alveolar rhabdomyosarcoma. J Clin Invest 1994;94:1235–42.
[17] Salisbury AJ, Macaulay VM. Development of molecular agents for IGF receptor targeting. Horm Metab Res 2003;35:843–9.
[18] Garcia-Echeverria C, Pearson MA, Marti A, Meyer T, Mestan J, Zimmermann J, et al. In vivo antitumor activity of NVP-AEW541-A novel, potent, and selective inhibitor of the IGF-IR kinase. Cancer Cell 2004;5:231–9.
[19] Scotlandi K, Manara MC, Nicoletti G, Lollini PL, Lukas S, Benini S, et al. Antitumor activity of the insulin-like growth factor-I receptor kinase inhibitor NVP-AEW541 in musculoskeletal tumors. Cancer Res 2005;65:3868–76.
[20] Calle EE, Rodriguez C, Walker-Thurmond K, Thun MJ. Overweight, obesity, and mortality from cancer in a prospectively studied cohort of U.S. adults. N Engl J Med 2003;348:1625–38.
[21] El-Serag HB, Petersen NJ, Carter J, Graham DY, Richardson P, Genta RM, et al. Gastroesophageal reflux among different racial groups in the United States. Gastroenterology 2004;126:1692–9.
[22] Tsai TF, Yauk YK, Chou CK, Ting LP, Chang C, Hu CP, et al. Evidence of autocrine regulation in human hepatoma cell lines. Biochem Biophys Res Commun 1988;153:39–45.
[23] Scharf JG, Schmidt-Sandte W, Pahernik SA, Ramadori G, Braulke T, Hartmann H. Characterization of the insulin-like growth factor axis in a human hepatoma cell line (PLC). Carcinogenesis 1998;19:2121–8.
[24] Ellouk-Achard S, Djenabi S, De Oliveira GA, Desauty G, Duc HT, Zohair M, et al. Induction of apoptosis in rat hepatocarcinoma cells by expression of IGF-I antisense c-DNA. J Hepatol 1998;29:807–18.
[25] Arteaga CL, Kitten LJ, Coronado EB, Jacobs S, Kull FC, Allred DC, et al. Blockade of the type l somatomedin receptor inhibits growth of human breast cancer cells in athymic mice. J Clin Invest 1989;84:1418–23.
[26] Hofmann F, Brueggen J, Capraro H-G, Cozens R, Evans DB, Fabbro D, et al. In vitro and in vivo profiling of selective and potent IGF-IR kinase inhibitors. Proc AACR 2003;44:3798.
[27] Aden DP, Fogel A, Plotkin S, Damjanov I, Knowles BB. Controlled synthesis of HBsAg in a differentiated human liver carcinoma-derived cell line. Nature 1979;282:615–6.
[28] Nakabayashi H, Taketa K, Miyano K, Yamane T, Sato J. Growth of human hepatoma cells lines with differentiated functions in chemically defined medium. Cancer Res 1982;42:3858–63.
[29] Ocker M, Alajati A, Ganslmayer M, Zopf S, Lüders M, Neureiter D, et al. The histone-deacetylase inhibitor SAHA potentiates proapoptotic effects of 5-fluorouracil and irinotecan in hepatoma cells. J Cancer Res Clin Oncol 2005;131:385–94.
[30] Detjen K, Murphy D, Welzel M, Farwig K, Wiedenmann B, Rosewicz S. Downregulation of p21(waf/cip-1) mediates apoptosis of human hepatocellular carcinoma cells in response to interferon-gamma. Exp Cell Res 2003;282:78–89.
[31] Höpfner M, Sutter AP, Gerst B, Zeitz M, Scherübl H. A novel approach in the treatment of neuroendocrine gastrointestinal tumors: targeting the epidermal growth factor receptor by gefitinib (ZD1839). Br J Cancer 2003;89:1766–75.

[32] Gillies RJ, Didier N, Denton M. Determination of cell number in monolayer cultures. Anal Biochem 1986;159:109–13.
[33] Höpfner M, Sutter AP, Beck NI, Barthel B, Maaser K, Jockers-Scherübl MC, et al. Meta-iodobenzylguanidine induces growth inhibition and apoptosis of neuroendocrine gastrointestinal tumor cells. Int J Cancer 2002;101:210–6.
[34] Nicholson DW, Ali A, Thornberry NA, Vaillancourt JP, Ding CK, Gallant M, et al. Identification and inhibition of the ICE/CED-3 protease necessary for mammalian apoptosis. Nature 1995;376:37–43.
[35] Lee D, Long SA, Murray JH, Adams JL, Nuttall ME, Nadeau DP, et al. Potent and selective non-peptide inhibitors of caspases-3 and -7. J Med Chem 2001;44:2015–26.
[36] Höpfner M, Maaser K, Theiss A, Lenz M, Sutter AP, Kashtan H, et al. Hypericin activated by an incoherent light source has photodynamic effects on esophageal cancer cells. Int J Colorectal Dis 2003;18:239–47.
[37] Decker T, Lohmann-Matthes ML. A quick and simple method for the quantitation of lactate dehydrogenase release in measurements of cellular cytotoxicity and tumor necrosis factor (TNF) activity. J Immunol Meth 1988;115:61–9.
[38] Sutter AP, Maaser K, Höpfner M, Barthel B, Grabowski P, Faiss S, et al. Specific ligands of the peripheral benzodiazepine receptor induce apoptosis and cell cycle arrest in human esophageal cancer cells. Int J Cancer 2002;102:318–27.
[39] Maaser K, Höpfner M, Jansen A, Weisinger G, Gavish M, Kozikowski AP, et al. Specific ligands of the peripheral benzodiazepine receptor induce apoptosis and cell cycle arrest in human colorectal cancer cells. Br J Cancer 2001;85:1771–80.
[40] Sutter AP, Maaser K, Barthel B, Scherübl H. Ligands of the peripheral benzodiazepine receptor induce apoptosis and cell cycle arrest in oesophageal cancer cells: involvement of the p38MAPK signaling pathway. Br J Cancer 2003;89:564–72.
[41] Höpfner M, Sutter AP, Huether A, Schuppan D, Zeitz M, Scherübl H. Targeting the epidermal growth factor receptor by gefitinib for treatment of hepatocellular carcinoma. J Hepatol 2004;41:1008–16.
[42] Gilmore AP, Valentijn AJ, Wang P, Ranger AM, Bundred N, O'Hare MJ, et al. Activation of BAD by therapeutic inhibition of epidermal growth factor receptor and transactivation by insulin-like growth factor receptor. J Biol Chem 2002;277:27643–50.
[43] Huether A, Höpfner M, Sutter AP, Grabowski P, Schuppan D, Scherübl H. Erlotinib induces cell cycle arrest and apoptosis in hepatocellular cancer cells and enhances chemosensitivity towards cytostatics. J Hepatol 2005;43:661–9.
[44] Oh SH, Lee BH. A ginseng saponin metabolite-induced apoptosis in HepG2 cells involves a mitochondria-mediated pathway and its downstream caspase-8 activation and Bid cleavage. Toxicol Appl Pharmacol 2004;194:221–9.
[45] Zhu BD, Yuan SJ, Zhao QC, Li X, Li Y, Lu QJ. Antitumor effect of Gefitinib, an epidermal growth factor receptor tyrosine kinase inhibitor, combined with cytotoxic agent on murine hepatocellular carcinoma. World J Gastroenterol 2005;11:1382–6.
[46] Huether A, Höpfner M, Baradari V, Schuppan D, Scherübl H. EGFR blockade by cetuximab alone or as combination therapy for growth control of hepatocellular cancer. Biochem Pharmacol 2005;70:1568–78.
[47] Ahmad T, Farnie G, Bundred NJ, Anderson NG. The mitogenic action of insulin-like growth factor I in normal human mammary epithelial cells requires the epidermal growth factor receptor tyrosine kinase. J Biol Chem 2004;279:1713–9.
[48] Lu Y, Zi X, Pollak M. Molecular mechanisms underlying IGF-I-induced attenuation of the growth-inhibitory activity of trastuzumab (Herceptin) on SKBR3 breast cancer cells. Int J Cancer 2004;108:334–41.
[49] Lu D, Zhang H, Koo H, Tonra J, Balderes P, Prewett M, et al. A fully human recombinant IgG-like bispecific antibody to both the epidermal growth factor receptor and the insulin-like growth factor receptor for enhanced antitumor activity. Biochem Pharmacol 2005;280:19665–72.
[50] Mitsiades CS, Mitsiades NS, McMullan CJ, Poulaki V, Shringarpure R, Akiyama M, et al. Inhibition of the insulin-like growth factor receptor-1 tyrosine kinase activity as a therapeutic strategy for multiple myeloma, other hematologic malignancies, and solid tumors. Cancer Cell 2004;5:221–30.
[51] Camirand A, Pollak M. Co-targeting IGF-1R and c-kit: synergistic inhibition of proliferation and induction of apoptosis in H 209 small cell lung cancer cells. Br J Cancer 2004;90:1825–9.
[52] Baserga R, Peruzzi F, Reiss K. The IGF-1 receptor in cancer biology. Int J Cancer 2003;107:873–7.
[53] LeRoith D, Roberts CT. The insulin-like growth factor system and cancer. Cancer Lett 2003;195:127–37.
[54] Sutter AP, Maaser K, Grabowski P, Bradacs G, Vormbrock K, Höpfner M, et al. Peripheral benzodiazepine receptor ligands induce apoptosis and cell cycle arrest in human hepatocellular carcinoma cells and enhance chemosensitivity to paclitaxel, docetaxel, doxorubicin and the Bcl-2 inhibitor HA14-1. J Hepatol 2004;41:799–807.
[55] Goldstein JC, Waterhouse NJ, Juin P, Evan GI, Green DR. The coordinate release of cytochrome c during apoptosis is rapid, complete and kinetically invariant. Nat Cell Biol 2000;2:156–62.
[56] Gogvadze V, Robertson JD, Zhivotovsky B, Orrenius S. Cytochrome c release occurs via Ca^{2+}-dependent and Ca^{2+}-independent mechanisms that are regulated by Bax. J Biol Chem 2001;276:19066–71.
[57] Liu B, Fan Z. The monoclonal antibody 225 activates caspase-8 and induces apoptosis through a tumor necrosis factor receptor family-independent pathway. Oncogene 2001;20:3726–34.
[58] Sheikh MS, Antinore MJ, Huang Y, Fornace AJ. Ultraviolet-irradiation-induced apoptosis is mediated via ligand independent activation of tumor necrosis factor receptor 1. Oncogene 1998;17:2555–63.
[59] Belka C, Marini P, Lepple-Wienhues A, Budach W, Jekle A, Los M, et al. The tyrosine kinase lck is required for CD95-independent caspase-8 activation and apoptosis in response to ionizing radiation. Oncogene 1999;18:4983–92.
[60] Bantel H, Engels IH, Voelter W, Schulze-Osthoff K, Wesselborg S. Mistletoe lectin activates caspase-8/FLICE independently of death receptor signaling and enhances anticancer drug-induced apoptosis. Cancer Res 1999;59:2083–90.
[61] Micheau O, Solary E, Hammann A, Dimanche-Boitrel MT. Fas ligand-independent, FADD-mediated activation of the Fas death pathway by anticancer drugs. J Biol Chem 1999;274:7987–92.
[62] Wesselborg S, Engels IH, Rossmann E, Los M, Schulze-Osthoff K. Ultraviolet-irradiation-induced apoptosis is mediated via ligand independent activation of tumor necrosis factor receptor 1. Blood 1998;93:3053–63.
[63] Gil J, Esteban M. The interferon-induced protein kinase (PKR), triggers apoptosis through FADD-mediated activation of caspase-8 in a manner independent of Fas and TNF-alpha receptors. Oncogene 2000;19:3665–74.
[64] Balachandran S, Roberts PC, Kipperman T, Bhalla KN, Compans RW, Archer DR, et al. Alpha/beta interferons

potentiate virus-induced apoptosis through activation of the FADD/caspase-8 death signaling pathway. J Virol 2000;74:1513–23.
[65] Morinaga S, Nakamura Y, Ishiwa N, Yoshikawa T, Noguchi Y, Yamamoto Y, et al. Expression of survivin mRNA associates with apoptosis, proliferation and histologically aggressive features in hepatocellular carcinoma. Oncol Rep 2004;12:1189–94.
[66] Grabowski P, Kühnel T, Mühr-Wilkenshoff F, Heine B, Stein H, Höpfner M, et al. Prognostic value of nuclear survivin expression in oesophageal squamous cell carcinoma. Br J Cancer 2003;88:115–9.